Available online www.jsaer.com

Journal of Scientific and Engineering Research, 2017, 4(8):11-19

Research Article

ISSN: 2394-2630
CODEN(USA): JSERBR

Temperature effect on the shunt resistance of a white biased silicon solar cell

Ibrahima Diatta[1], Marcel SitorDiouf[1], Hameth Yoro Ba[2], Youssou Traore[1,2], Ousmane Diasse[1], Seydou Faye[1], Gregoire Sissoko[1]

[1]Laboratoire des Semi-conducteurs et d'Energie Solaire, Faculté des Sciences et Techniques, Université Cheikh AntaDiop, Dakar, Sénégal
[2]Ecole Polytechnique de Thiès, Sénégal

Abstract The shunt resistance is an important electrical parameter in the operation of the solar cell. It can be determined from the photocurrent-photovoltage characteristic for the large values of the recombination velocity of the minority charge carriers at the junction. The photocurrent - photovoltage characteristic is the photocurrent evolution as a function of the photovoltage with as parameter the recombination velocity of the minority charge carriers at the junction. The object of this work is the determination of the shunt resistance knowing the recombination velocity of the minority charge carriers at the junction initiating the short circuit. The presence of the temperature influences the parameters of the solar cell and will allow to study its impact on the shunt resistance of the solar cell subjected to a polychromatic illumination and in static regime. Thus, the minority charge carriers density is obtained from the continuity equation, which allows the determination of the expressions of the photocurrent and of the photovoltage. From the photocurrent - photovoltage characteristic, the shunt resistance is determined and then studied as a function of the temperature.

Keywords Silicon Solar Cell - Photocurrent – Shunt Resistance – Temperature

Introduction

The manufacturing defects of the solar cells are characterized the shunt resistance. This resistance resembles an alternating current path in favor of the photocurrent [1-3]. In static regime [4-6] as in dynamic frequency regime [7-9], the shunt resistance can be studied.

Numerous methods have been used for the determination of the shunt resistance. Among these methods, we have the simple models and double exponential [8], the numerical method [9-10], the method of the characteristic (I-V) using the grain size (g) and the recombination velocity to grain boundaries [4]. In our study, we consider the photocurrent - photovoltage characteristic with as parameter the recombination velocity of the minority charge carriers at the junction initiating the short circuit. Thus, under these conditions, an equivalent electrical circuit corresponding to the short-circuit operation of the solar cell, is proposed which makes it possible to determine the shunt resistance. The application of the temperature allows to study its effect on the shunt resistance of the silicon solar cell under polychromatic illumination and in static regime.

Theory

In this study we consider a type of solar cell n^+-p-p^+[11] under polychromatic illumination. The structure of this solar cell is shown in Figure 1:

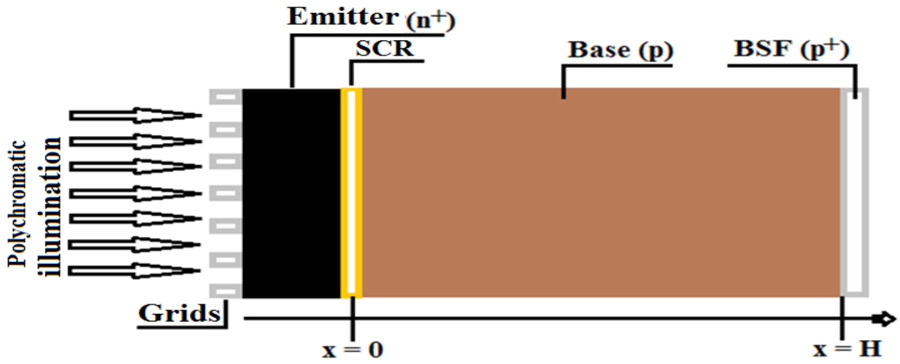

Figure 1: Silicon solar cell n+pp+ type

When the solar cell is illuminated by polychromatic light various phenomena such as the creation of electron-hole pairs, the diffusion of the minority charge carriers in the base as well as the recombination can occur. The whole of these phenomena is governed by an equation called: continuity equation which is relative to the density of excess minority carriers in the base. It is represented by Equation 1:

$$\frac{\partial\delta(x)}{\partial x^2}-\frac{\delta(x)}{L(T)^2}=-\frac{G(x)}{D(T)} \quad (1)$$

In this equation, D (T) represents the diffusion coefficient which is a function of temperature according to equation (2):

$$D(T)=\mu(T)\frac{k_b}{q}T \quad (2)$$

$\mu(T)$characterizes the mobility of electrons **[**12-13**]** and is a function of temperature, its expression is given by:

$$\mu(T)=1,43.10^9T^{-2,42}cm^2V^{-1}s^{-1} \quad (3)$$

k_b is the Boltzmann constant, q the elementary charge of the electron and T the temperature.
L(T) represents the diffusion length which depends on the diffusion coefficient according to the relationship:

$$\left(L(T)\right)^2=\tau D(T) \quad (4)$$

τ is the lifetime of the minority charge carriers photogenerated in the base
G(x) represents the rate of generation of the minority load carriers which depends on the depth in the base according to relation [14]:

$$G(x)=\sum_{i=1}^{3}a_ie^{-b_ix} \quad (5)$$

The coefficients ai and bi are obtained from the tabulated values of the radiation under A.M1.5 [15]. These coefficients are given by:
$a_1=6,13.10^{20}$ cm^{-3}/s; $a_2=0,54.10^{20}cm^{-3}/s$; $a_3=0,0991.10^{20}cm^{-3}/s$; $b_1=6630cm^{-1}$; $b_2=1000cm^{-1}$;
δ(x) represents the density of minority charge carriers in the base, its expression is given by the resolution of equation (1):

$$\delta(x,T)=A\cosh\left(\frac{x}{L(T)}\right)+B\sinh\left(\frac{x}{L(T)}\right)+\sum_{i=1}^{3}\frac{a_i(L(T))^2}{D(T)\left[(L(T))^2(b_i)^2-1\right]}e^{-b_ix} \quad (6)$$

The expressions of A and B are determined from the boundary conditions **[**16-17**]:**

- at the junction*(x=0)*

$$\left.\frac{\partial\delta(x,T)}{\partial x}\right|_{x=0} = \frac{S_f}{D(T)}\delta(x,T)\Big|_{x=0} \qquad (7)$$

- at the back surface (*x=H*):

$$\left.\frac{\partial\delta(x,T)}{\partial x}\right|_{x=H} = -\frac{S_b}{D(T)}\delta(x,T)\Big|_{x=H} \qquad (8)$$

S_f represents the recombination velocity of the minority charge carriers at the junction. It characterizes the operating point of the solar cell but also the minority carrier flux at the junction **[16-17].** Sb is the recombination velocity of the minority charge carriers at the back surface **[**17**].** The expression of the density of the minority carriers makes it possible to access the photocurrent and the photovoltage according to the equations:

$$J_{ph}(S_f,T) = qD(T)\left.\frac{\partial\delta(S_f,T)}{\partial x}\right|_{x=0} \qquad (9)$$

$$V_{ph}(S_f,T) = V_T \ln\left[\frac{N_b}{\left(n_i^2(T)\right)}\delta(0,S_f,T)+1\right] \qquad (10)$$

Jph represents the photocurrent density, Vph the photovoltage and N_b the doping rate.
$n_i(T)$ is the intrinsic density of the minority carriers, its depends on the temperature according to the relation **[**18**]**:

$$n_i = C.T^{\frac{3}{2}} \exp\left(-\frac{E_g}{2.k_b.T}\right) \qquad (11)$$

With C a constant equal to $3.87.10^{16}$ cm^{-3} $K^{-3/2}$ and Eg the gap energy. This energy is the difference between the energy of the conduction band E_c and that of the valence band E_v. It is equal to $1.12x1.6x10^{-19}$ J for the silicon.
V_T represents the thermal voltage given by:

$$V_T = \frac{k_b}{q}T \qquad (12)$$

Results and Discussions

Equations (9) and (10) yielded the following profiles:

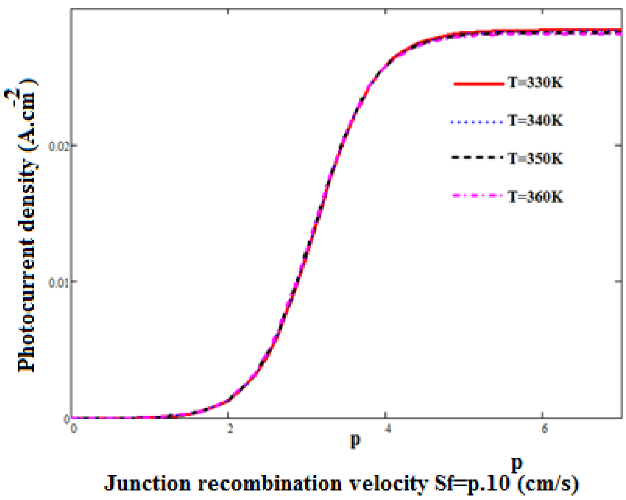

Figure 2: Photocurrent Density as a function of the recombination velocity of the minority charge carriers at the junction for different values of the temperature

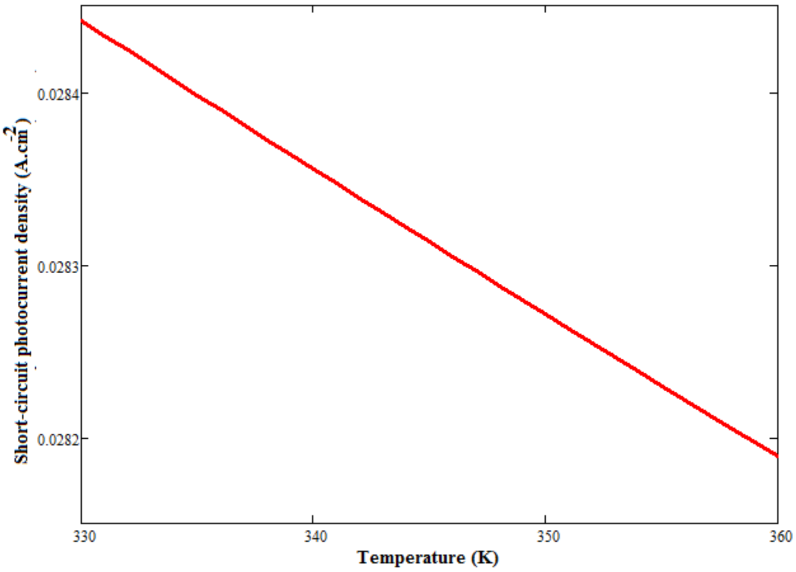

Figure 3: Short-circuit photocurrent density as a function of temperature

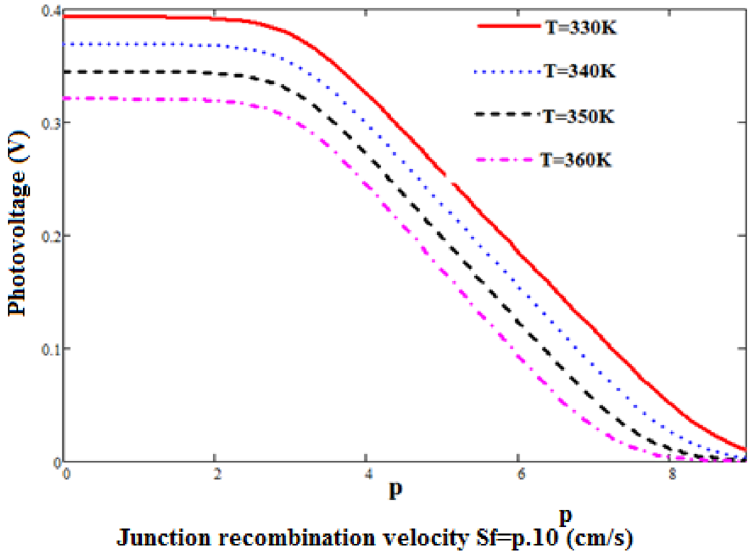

Figure 4: Photovoltage as a function of the recombination velocity of the minority charge carriers at the junction for different temperature values

Figure 2 shows a weak photocurrent in the vicinity of the open circuit (at the low Sf values): The minority carriers are blocked at the junction because they lack energy to cross the potential barrier located at the junction. When Sf increases, the minority charge carriers cross the junction and the photocurrent increases to reach a maximum value at the large Sf values: This is the short-circuit current. We also observe a decrease in the short-circuit current when the temperature increases with very low sensitivity. This observation is confirmed by figure 3. Indeed, at the large values of Sf, the flux of the minority charge carriers at the junction is maximal, so there remains a small amount of the minority charge carriers that can be undergo by the temperature effect. Everything happens as if the increase of Sf tends to inhibit the process umklapp **[**19-21**],** that is to say a decrease in the resistivity of the material. On the other hand, at the low values of Sf (in the vicinity of the short-circuit), the minority charge carriers are blocked at the junction leading to a maximum photovoltage: this is the open circuit voltage (figure 4). It decreases when Sf increases to cancel out in the vicinity of the short circuit. Indeed, when Sf increases the amount of stored minority charge carriers decreases which results in a decrease of photovoltage. We also observe that increasing the temperature decreases the open circuit voltage with a sharper sensitivity: Here we have the process umklapp **[**19-21**]** which results in an increase in the resistivity of the material. The observations described above are confirmed in the Photocurrent - photovoltage characteristic. It is represented by figure 5.

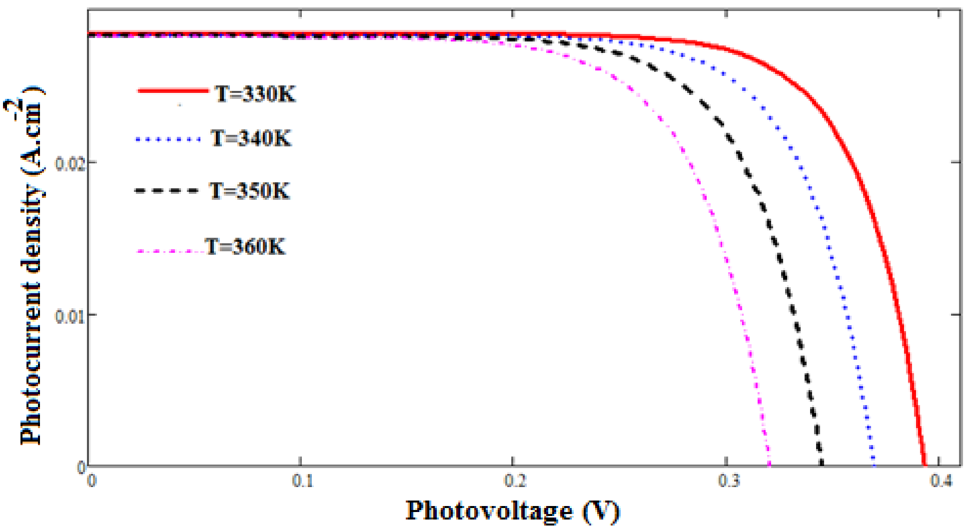

Figure 5: Photocurrent - Photovoltage characteristic for different temperature values

Study of the shunt resistance

The shunt resistance represents the set of leakage currents within the solar cell. It models the imperfections at the edge of the solar cell and on the space charge area. It may be related to the recombination velocity at the junction. For its determination, we consider the low photovoltage values of the Photocurrent - photovoltage characteristic. This part of the curve corresponds to the short-circuit situation. Under these circumstances, the characteristics to the solar cell are comparable to a short-circuit current generator in parallel with the shunt resistance and a load resistance [27].We represent in Figure 6 the equivalent circuit of the solar cell working in the vicinity of the short circuit [22-26]:

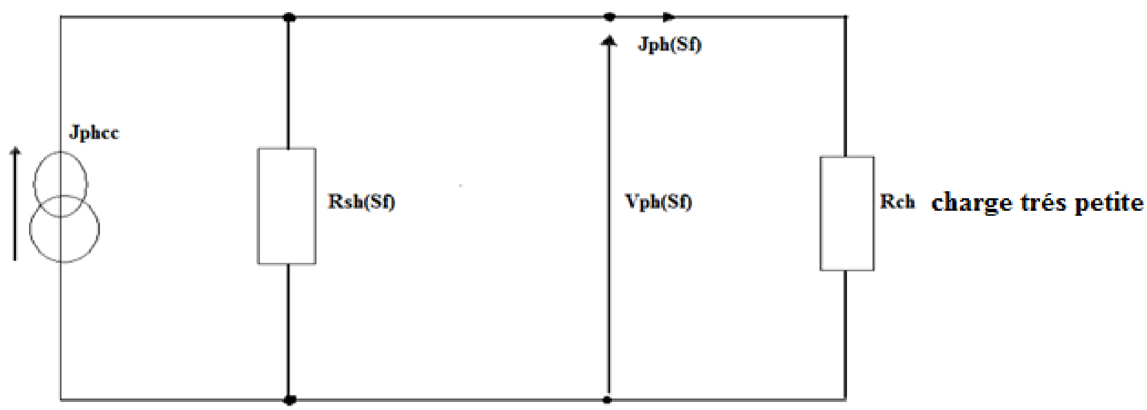

Figure 6: Electrical equivalent circuit of the solar cell unit when it operates practically in short-circuit

Using the circuits of figure 6, the shunt resistances can be expressed as:

$$R_{sh}(S_f,T) = \frac{V_{ph}(S_f,T)}{J_{phcc}(T) - J_{ph}(S_f,T)} \quad (13)$$

Jphcc is short-circuit photocurrent density. Jph (Sf, T) and Vph (Sf, T) respectively represent the photocurrent density and the photovoltage. Rch is a low resistance of load producing large values of Sf and Rsh (Sf, T): shunt resistance. From expression 13, we represent in Figure 7 the profile of the shunt resistance as a function of the recombination velocity of the minority charge carriers at the junction for different values of the temperature.

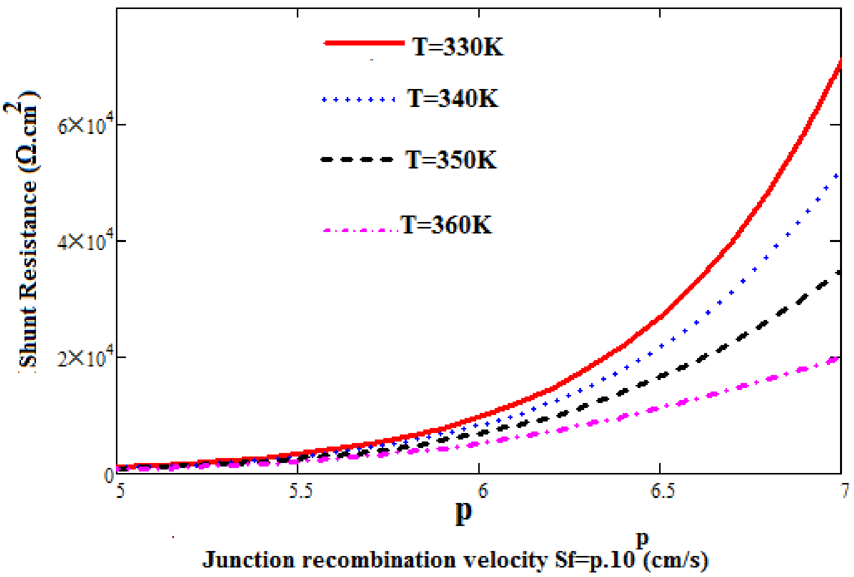

Figure 7: Shunt resistance as a function of the recombination rate at the junction for different temperature values

La figure 7 shows an increase in the shunt resistance with the recombination velocity of the minority charge carriers at the junction. Indeed, when Sf increases the flow of minority load carriers increases, which means that the current available for the external load becomes large and taking account of expression 13, an increase in the shunt resistance is observed. We also find that an increase in temperature leads to a decrease in the shunt resistance. Thus, with the process umklapp [19-21] in high temperature, the resistivity of the material increases which causes a reduction in the current available for the external load and consequently a decrease in the Shunt resistance.

Determination of the shunt resistance from the recombination velocity of the minority charge carriers initiating the short circuit (Sfcc)

The expression of Sfcc is obtained from the resolution of Equation 14 **[28, 29]:**

$$Jph(S_f, T) - Jphcc(T) = 0 \tag{14}$$

Thus, we obtain

$$Sfcc(T) = \frac{L(T)\sum_{i=1}^{3} K(T)\left[L(T)E(T) - \mathrm{M(T)}\mathrm{b}_i\, D(T)\right] - \gamma_a(T)D(T)M(T)}{L(T)\left[\gamma_a(T)M_1(T) + \sum_{i=1}^{3} K(T)M(T)\right]} \tag{15}$$

Avec,

$$E(T) = L(\mathrm{T})\left[S_b - \sum_{i=1}^{3} b_i D(T)\right] e^{-b_i H}$$

$$M(T) = L(T)S_b \cosh\left(\frac{H}{L(T)}\right) + D(T)\sinh\left(\frac{H}{L(T)}\right)$$

$$\gamma_a(T) = L(\mathrm{T})\left[\frac{Jphcc(T)}{qD(T)} - \sum_{i=1}^{3} K(T)b_i\right]$$

$$\mathrm{M}_1(T) = L(\mathrm{T})\mathrm{S}_b \sinh\left(\frac{H}{L(T)}\right) + D(T)\cosh\left(\frac{H}{L(T)}\right)$$

Referring to figure 7, the values of the temperature have allowed, after their introduction in equation 15, to obtain the values of Sfcc. These latters, projected at the level of the curves of figure 7, have made it possible to determine the shunt resistance for different temperature values. The results are recorded in Table 1.

Table 1: Sfcc and Rsh values for different temperature

T(K)	Sfcc(cm/s)	Rsh(Ω.cm²)
330	$3{,}115.10^{6}$	7250,9
340	$3{,}210.10^{6}$	6730,5
350	$3{,}322.10^{6}$	6012,2
360	$3{,}452.10^{6}$	4502,3

Table 1 shows that the temperature increases the recombination velocity of the minority carriers at the junction initiating the short circuit. Thus, more the temperature increases, more the resistance of the material increases (with the umklapp process [19-21]), which means that the short-circuit situation is difficult to reach for high temperatures and confirms the decrease of the shunt resistance. In order to observe this phenomenon, we represent in figure 8 the profile of the shunt resistance as a function of the temperature.

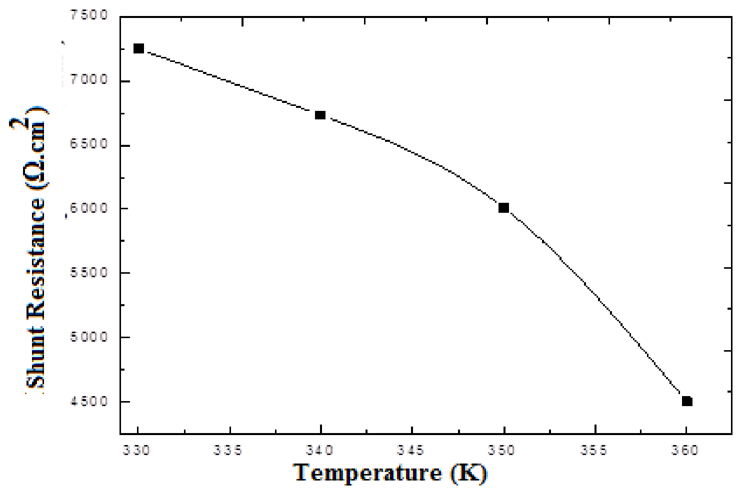

Figure 6: Shunt resistance as a function of temperature

Conclusion

In this work, the expressions of photocurrent and photovoltage are determined from the density of minority charge carriers at the junction. The Photocurrent - Photovoltage characteristic is represented for different values of the temperature. The study showed a slight decrease in the short-circuit photocurrent and a considerable drop in the open circuit voltage. From the Photocurrent - photovoltage characteristic, the shunt resistance is determined and then studied for different temperature values. From the expression of the recombination velocity of the minority charge carriers at the junction initiating the short-circuit (Sfcc) the values of the shunt resistance for different temperatures are presented and showed a decrease in the shunt resistance and an increase of Sfcc when the temperature increases.

References

[1]. M.Bashahu and A. Habyarimana. Review and test of methods for determination of the solar cell series resistance. Renewable Energy, 6,2, pp. 127-138, (1995).

[2]. M.K. El- Adawi and I.A. Al-Nuaim. A method to determine the solar cell series resistance from a single I-V characteristic curve considering its shunt resistance-new approach. Vacuum, 64, pp: 33-36, (2002).

[3]. K. Bouzidi, M. Chegaar and A. Bouhemadou. Solar cells parameters evaluation considering the series and shunt resistance. Solar Energ. Mater. Solar Cells, 91, pp.1647-1651, (2007).

[4]. S. Mbodji, I. Ly, H. L. Diallo, M.M. Dione, O. Diasse and G. Sissoko. Modeling Study of N^+/P Solar Cell Resistances from Single I-V Characteristic Curve Considering the Junction Recombination Velocity (Sf). Research Journal of Applied Sciences, Engineering and Technology 4, 1, pp. 1-7, 2012.

[5]. J. Lauwaert, K. Decock, S. Khelifi, M. Burgelman**.** A simple correction method for series resistance and inductance on solar cell admittance spectroscopy**.** Solar Energy Materials & Solar Cells, 94, pp. 966–970, (2010).

[6]. H. Bayhan, A. S. Kavasglu. **A**dmittance and impedance spectroscopy on Cu(In,Ga)Se_2 solar cells**.** Turk. J. Phys., 27, pp. 529-535, (2003).

[7]. J. H. Scofield. Effects of series resistance and inductance on solar cell admittance measurements**.** Solar Energy Materials and Solar Cells, 37 (2), pp: 217-233, May 1995.

[8]. P. Singh, S.N. Singh, M. Lal, M. Husain. Temperature dependence of I–V characteristics and performance parameters of silicon solar cell**.** Solar Energy Materials & Solar Cells, 92, pp. 1611–1616, (2008).

[9]. F. Ghani, M. Duke. Numerical determination of parasitic resistances of a solar cell using the Lambert W-function**.** Solar Energy, 85, pp. 2386–2394, (2011).

[10]. F. Ghani, M. Duke, J. Carson. Numerical calculation of series and shunt resistances and diode quality factor of a photovoltaic cell using the Lambert W-function**.** Solar Energy, 91 pp.422–431, (2013).

[11]. N. Le Quang, M. Rodot, J. Nijs, M. Ghannam, and J. Coppye. Spectral response of high-efficiency multicrystalline silicon solar cells. J. Phys. III, (France) pp. 1305-1316.

[12]. M. Kunst, and A. Sanders. Transport of Excess Carriers in Silicon Wafers. Semiconductor Science and Technology, 7, pp. 51-59. (1992)

[13]. D. K. Schroder, J.D. Whitfield, and C.J. Varker. Recombination Lifetime Using the Pulsed MOS Capacitor. IEEE Transactions on Electron Devices , 31, pp. 462-467,(1984)

[14]. J. Furlan and S. Amon. Approximation of the carrier generation rate in illuminated silicon. Solid State Electron. 28, pp.1241–43,(1985).

[15]. S. N. Mohammad. An alternative method for the performance analysis of silicon solar cells. J. Appl. Phys. 61,2, pp.767-777, (1987)

[16]. H.L. Diallo, A. S. Maiga, A. Wereme, and G. Sissoko. New approach of both junction and back surface recombination velocities in a 3D modelling study of a polycrystalline silicon solar cell. Eur. Phys. J. Appl. Phys. 42, pp. 203–211, (2008).

[17]. G. Sissoko, C. Museruka, A. Corréa, I. GAYE, A. L. Ndiaye. Light spectral effect on recombination parameters of silicon solar cell. **»**, World Renewable Energy Congress 3, Denver-USA pp. 1487-1490, (1996).

[18]. C. D. Thurmond, **«**The standard thermodynamic functions for the formation of electron and hole in Ge, Si,GaAs and GaP**.** J. Electrochem. Soc, vol. 122, pp 133-41, (1975).

[19]. R. Berman. Thermal Conductivity of Dielectric Crystals: The Umklapp**.** Nature 168, pp. 277-280, (1951)

[20]. H.B.G. Casimir. Note on the Conduction of Heat in Crystals. Physica 5, pp. 495-500, (1938)

[21]. R.E.B. Makinson. The Thermal Conductivity of Metals. Mathematical Proceedings of the Cambridge Philosophical Society, 34, pp. 474-497, (1938)

[22]. M.M. Dione, H. Ly Diallo, M. Wade, I. Ly, M. Thiame, F. Toure, A. G.Camara, N. Dieme, Z. N. Bako, S. Mbodji, F. I Barro, G. Sissoko. Determination of the shunt and series resistances of a ver-ticalmulti junction solar cell under constant multispec-tral light**.** 26th European Photovoltaic Solar Energy Conference and Exhibition, pp. 250-254, (Hamburg, 2011),

[23]. M.L. Samb, S. Sarr, S. Mbodji, S. Gueye, M. Dieng and G. Sissoko. Etude en modélisation à 3-D d'une photopile au silicium en régime statique sous éclairement multispectrale : détermination des paramètres électriques**.** J. Sci.Vol. 9**,** 4, pp. 36-50, (2009)

[24]. F. I. Barro, S. Gaye, M. Deme, H. L. Diallo, M. L. Samb, A. M. Samoura, S. Mbodji and G. Sissoko. In-fluence of grain size and grain boundary recombination velocity on the series and shunt resistances

of a poly-crystalline silicon solar cell. Proceedings of the 23rd European Photovoltaic Solar Energy Conference, pp. 612-615, (2008),

[25]. A. Dieng, A. Diao, A.S. Maiga, A. Dioum, I. Ly, G. Sissoko. A Bifacial Silicon Solar Cell Parameters Determination by Impedance Spectroscopy. Proceedings of the 22nd European Photovoltaic Solar Energy Conference and Exhibition pp.436-440, (2007)

[26]. O. Sow, I. Zerbo, S. Mbodji, M. I. Ngom, M. S. Diouf, G. Sissoko. Silicon solar cell under electromagnetic waves in steady state: Electrical parameters determination using the I-V and P-V characteristics. International Journal of Science, Environment and Technology, 1, 4, pp. 230-246, (2012)

[27]. Th. Flohr and R. Helbig. Determination of minority-carrier lifetime and surface recombination velocity by Optical-Beam-Induced- Current measurements at different light wavelengths. J. Appl. Phys., 66, 7, pp 3060 – 3065, (1989)

[28]. I. Ly, M. Ndiaye, M. Wade, Ndeye Thiam, S. Gueye, G. Sissoko. Concept of Recombination Velocity Sfcc At The Junction of A Bifacial Silicon Solar Cell, In Steady State, Initiating The Short-Circuit Condition. Research Journal of Applied Sciences, Engineering and Technology, 5,1, pp. 203-208, (2013).

[29]. M. S. Diouf, I. Ly, M. Wade, I. Diatta, Y. Traore, M. Ndiaye, G. Sissoko. The Temperature Effect on The Recombination Velocity at the junction Initiating The Short-Circuit Condition (Sfcc) of a Silicon Solar Cell under External Electric Field. Journal of Scientific and Engineering Research (JSAER), 3,6, pp. 410-420, (2016)